J Mater Sci (2015) 50:6260–6267
DOI 10.1007/s10853-015-9146-2

HVPE growth of self-aligned GaN nanorods on *c*-plane, *a*-plane, *r*-plane, and *m*-plane sapphire wafers

Sung Ryong Ryu[1,2] · S. D. Gopal Ram[1] · Yang Hae Kwon[1] · Woo Chul Yang[2] · Seung Hwan Kim[2] · Yong Deuk Woo[5] · Sun Hye Shin[4] · Tae Won Kang[1,3]

Received: 24 December 2014 / Accepted: 2 June 2015 / Published online: 24 June 2015

Abstract Herein, we report the self-aligned growth of GaN nanorods on different orientations of sapphire like *c*-, *a*-, *r*- and *m*-plane substrates by hydride vapor phase epitaxy. Vertical *c*-axis orientation of GaN NRs is obtained on *c*-plane [0001] and *a*-plane $[11\bar{2}0]$ sapphire and a skew or inclined NRs on *r*-plane, and inclined intertwined but self-aligned NR array was formed on *m*-plane sapphire. GaN (002) and (004) peaks were obtained on *c*- and *a*-plane sapphire, whereas (110), (103), and (103) only were observed on *r*- and *m*-planes, respectively. In the case of *r*- and *m*-plane-grown GaN, A_1 transverse optical mode is dominant, and the A_1 longitudinal optical mode is suppressed. Conversely, in the case of *c*- and *a*-plane, it is reversed. The probable reason is the optical mode vibrations difference along the differently inclined NRs surfaces. In addition, the specimen exhibits surface optical modes too. The optical behavior of GaN NR on *m*-sapphire shows an intensity variation when measured in different angular rotations of the specimen by photoluminescence which is because of the higher area of excitation in the case of axial surfaces and lower area of excitation in radial surface. Their epitaxial crystallographic relationship with the substrates and the reasons for the self-aligned orientations are discussed. The anomalies found in the optical behavior are attributed to Raman antenna effect and so on. The self-aligned intertwined GaN NRs find suitable applications in polarizer.

Introduction

GaN is one of the inevitable candidates in the III-nitride family in optoelectronic applications [1] such as light emitting diodes [2], laser diodes, etc., [3]. GaN nanorods (NR) have more advantages than their 2D counterpart (thin films) like having larger surface area due to their high aspect ratio, single crystalline nature, and low defect density which are desirable for solid-state devices. Since tilt and twist do not generate more defects, the need for coalescence process is overcome [4]. Because of the unusual anisotropic optical properties, they are suitable for applications such as

✉ Tae Won Kang
twkang@dongguk.edu

Sung Ryong Ryu
ysmrsr@naver.com

S. D. Gopal Ram
gopalramb4u@gmail.com

Yang Hae Kwon
sige@dongguk.edu

Woo Chul Yang
wyang@dongguk.edu

Seung Hwan Kim
optical88@naver.com

Yong Deuk Woo
Wooyongd@woosuk.ac.kr

Sun Hye Shin
almien2004@naver.com

[1] Quantum-Functional Semiconductor Research Center, Dongguk University, 26,3 Pil-dong, Jung gu, Seoul 100-715, Korea

[2] Department of Physics, Dongguk University, Seoul 100-715, Korea

[3] Clean Energy and Nano Convergence Centre, Hindustan University, Chennai 600 016, India

[4] Soft-Epi Inc., 240 Opo-ro, Opo-eup, Gwangju-Si, Gyeonggi-do, Korea

[5] Department of Mechanical and Automotive Engineering, Woosuk University, Chonbuk 565-701, Korea

polarization sensitive photodetectors and optical modulators [5]. For the growth of such twisted or inclined growth of GaN NR, non-polar or semipolar orientation planes of sapphire could be a good choice, since it is cheaper and easily available in larger area than the other suitable counterparts such as $LiAlO_2$, ZnO, and SiC. In addition, sapphire is more preferable because it is chemically inert, optically transparent, and thermally stable [6]. It has a better thermal conductivity and hence can reduce the defect incorporation to a better extent than the rest of the materials of choice of substrate [7, 8]. HVPE method very well demonstrates to be a cost-effective and versatile method for the growth of NRs, rather than MOCVD or MBE, etc. [9]. Very few reports have been found on the growth of non-polar and semipolar GaN NRs, that too by sophisticated MOCVD method [10]. But in this report, we demonstrate the growth of GaN NRs in all orientations by the simple catalyst-free HVPE method, without any special surface treatment for the nucleation or growth. In this work, the growth on *m*-plane sapphire has yielded a self-aligned c-axis orientation and a semipolar epitaxial interface with that of sapphire. GaN has a band gap of 3.4 eV, and hence, it can absorb in the UV range and is suitable for UV polarizer applications. The difference in the orientations very well replicate in the optical properties, which is analyzed by Raman spectroscopy. The Photoluminescence (PL) is measured by rotating the specimen, to identify the optical effect of the NRs inclined in different orientations. An increase in intensity is found at some angles in analogous with the anisotropic property of NR.

Materials and methods

The HVPE equipment used for the growth of GaN NRs is divided into three zones. The first zone maintained at around 800 °C favors the chemical reaction of Ga metal with HCl gas to form $GaCl_3$ and hydrogen.

$$Ga + HCl_{(g)} = GaCl_3 + H_2, \quad (1)$$

$$GaCl_3 + NH_3 = GaN + 3HCl. \quad (2)$$

The second zone is the GaN forming zone. In this zone, NH_3 dissociates to provide nitrogen atoms. In order to crack H_2 from ammonia, a higher temperature than the reaction zone around 1000 °C is needed. The $GaCl_3$ formed in the first zone reacts with nitrogen to form GaN [11, 12]. The growth of the GaN rods takes place in the third zone. For the growth of GaN NR, the third zone was maintained at a temperature of 800 °C. The optimum growth temperatures for the GaN film and NRs arrays are found be 1100 and 800 °C, respectively. The growth conditions such as temperature, zone, and gas flow rates were fixed in a several number of trial experiments [13]. The same growth conditions were used for all the cases of [0001] *c*-plane, $[11\bar{2}0]$ *a*-plane, $[1\bar{1}02]$ *r*- plane, and $[1\bar{1}00]$ *m*-plane sapphire.

Analysis and results

The prepared specimens were studied by X-ray diffraction (XRD), scanning electron microscopy (SEM), transmission electron microscopy (TEM), Raman and PL, etc. The top-view and the cross-sectional SEM images of the GaN NRs on different orientations of sapphire substrates along with their schematics of the GaN NRs grown along the orientations of Sapphire (a) [0001] *c*-plane, (b) $[11\bar{2}0]0$ *a*-plane, (c) $[1\bar{1}02]$ *r*-plane, and (d) $[10\bar{1}0]$ *m*-plane are shown in Fig. 1. The *c*- and *a*-plane sapphire substrates get the vertically aligned *c*-axis [0001] GaN NRs. But the *r*- and *m*-planes form tilted skew and inclined intertwined orientations, respectively. Fig. 1c, d show both the original and 90° rotated schematics for a clear illustration. The tilted skew NRs (Fig. 1c) inclined in two different orientations could be seen in the case of $[1\bar{1}02]$ *r*-plane sapphire. An inclined intertwined alignment is observed both from lateral and top view of (d) $[10\bar{1}0]$ *m*-plane sapphire. XRD pattern in Fig. 2 illustrates the origination of the different peaks of GaN dominantly on different substrates. From the TEM, from Fig. 3, it was ascertained that the rods grown on *c*- and *m*-plane sapphire planes primarily are c-axis oriented.

The optical properties of GaN NRs were analyzed by Raman spectroscopy and PL, respectively. Raman measurement was done using *Nanobase XperRam 200* instrument. The laser used was 532-nm diode-pumped solid-state laser with 0.7 mW power. The PL was measured using He–Cd laser (325 nm). Figure 4 depicts Raman shift of all GaN NRs grown on *a*-, *c*-, *r*-, and *m*-plane sapphire. The surface optical modes (SO) are found in all the cases. But the vertically aligned and inclined NRs differ in their optical property by exhibiting either longitudinal optical (LO) or transverse optical (TO) of A_1 phonon modes. Figure 5 represents the azimuth-dependent PL performance of the GaN NRs grown on *m*-plane sapphire. The PL was measured along 30°–300° in steps of 90°. Among them, an increased intensity is found along 30° and 210° than the rest. Similarly, when the azimuth-dependent PL spectra of *c*-plane and *m*-plane sapphire-grown samples are compared, an azimuth-dependent sinusoidal increase and decrease of intensity was found in the *m*-plane-grown GaN NRs which was absent in the *c*-plane-grown GaN NR. Figure 6 illustrates this comparison. The probable reasons are discussed in the forthcoming sections.

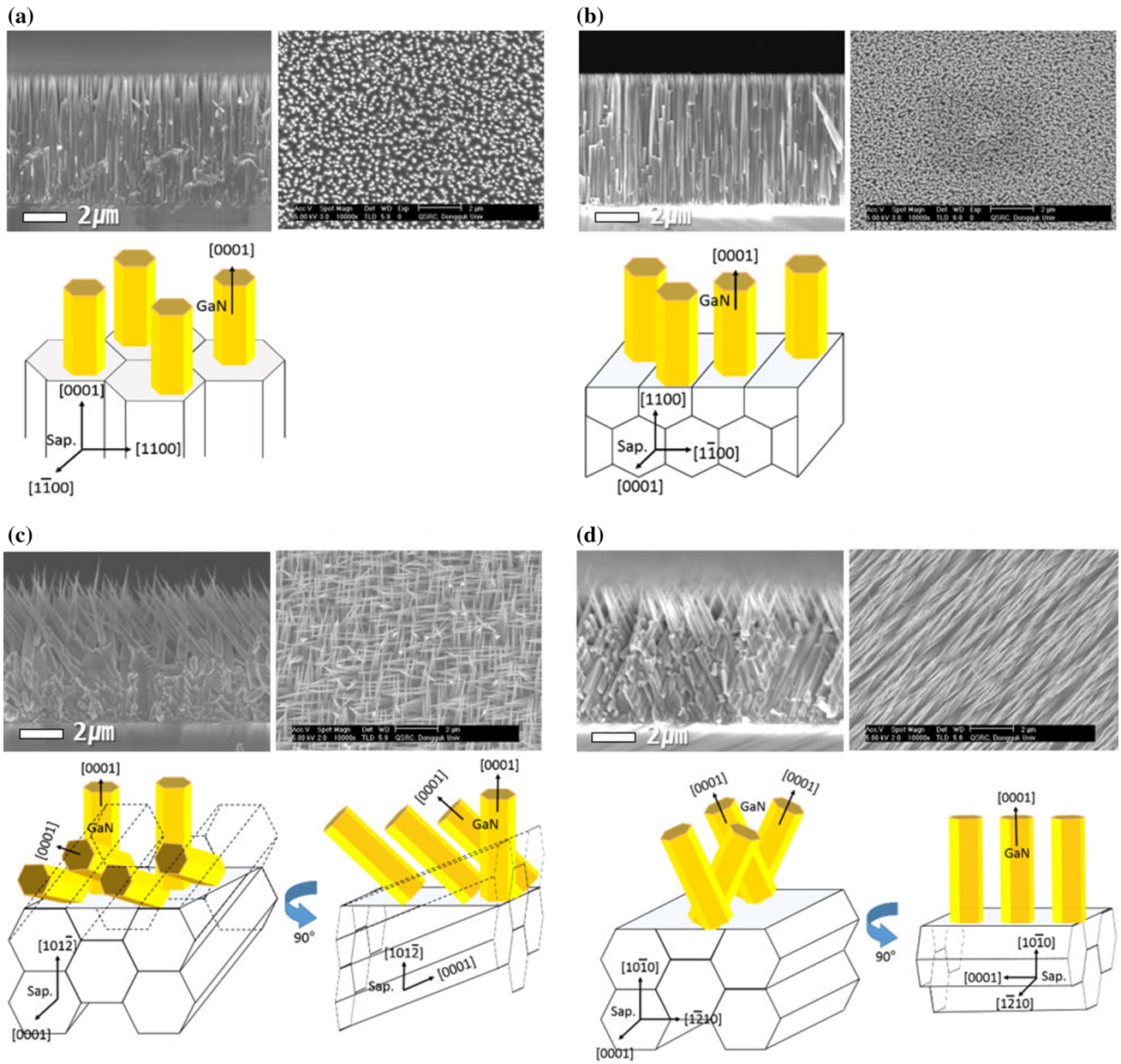

Fig. 1 SEM images of GaN nanorods grown on the **a** *c*-plane, **b** *a*-plane, **c** *r*-plane, and **d** *m*-plane sapphire substrates by HVPE method. The orientations are inclined in *r*-plane and *m*-plane, whereas they are vertical in the case of *c*- and *a*-plane. Schematic showing the epitaxial relationship of the GaN nanorods grown along various epitaxial orientations on different substrates

Discussion

Epitaxial relationship

The epitaxial relationship of *c*-plane $[0001]_{GaN}$ on *c*-plane $[0001]_{Sapphire}$ is widely studied and understood and therefore, is clearly known. In this report, we focus on the other orientations of sapphire substrates importantly. For a comparison, the characteristic *c*-axis-grown conventional polar [0001] GaN will be taken as a reference. In the case of *a*-plane sapphire, a N-rich or Ga-poor conditions on the surface during growth result in the formation of *a*-plane GaN grains elongated along the *c*-axis. The *a*-plane GaN epilayers when grown at higher temperatures lead to increased Ga desorption which results in N-rich condition [10]. Non-polar *a*-plane is inherently anisotropic along the two in-plane directions [1–100] (*m*-axis) and [0001] *c*-axis. Density functional theory (DFT) calculations, as reported by A. Lotsari et al. (2014), show large anisotropy in the diffusion barriers along and direction perpendicular to the *c*-axis under N-rich growth conditions on the N-stabilized surface. On the *a*-plane surface, the Ga adatoms exhibit

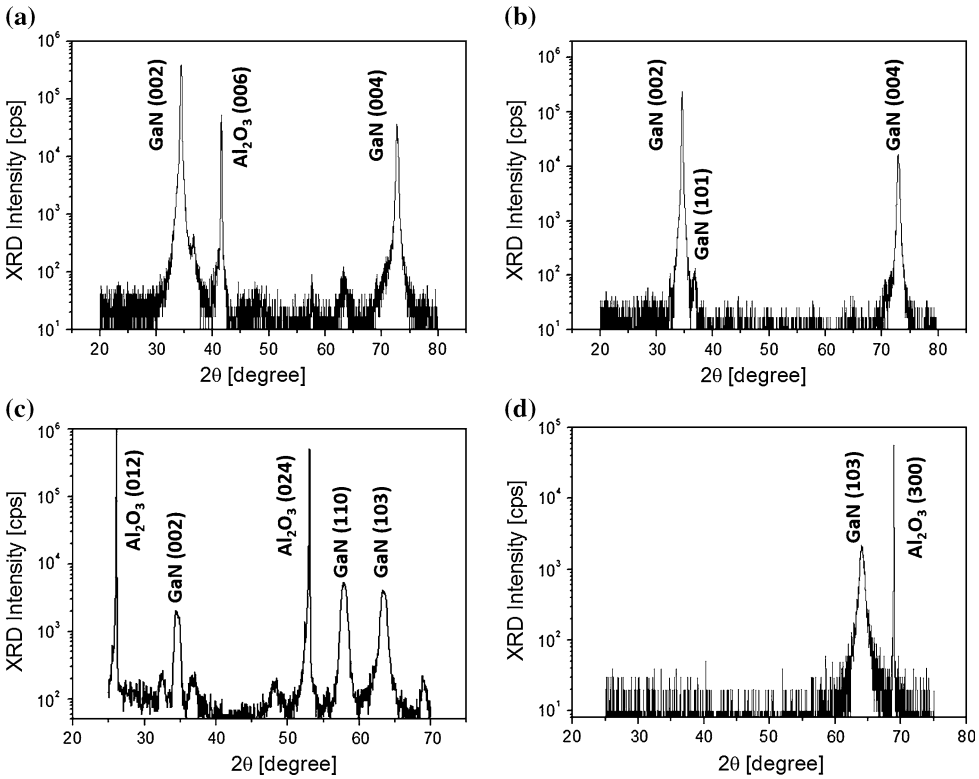

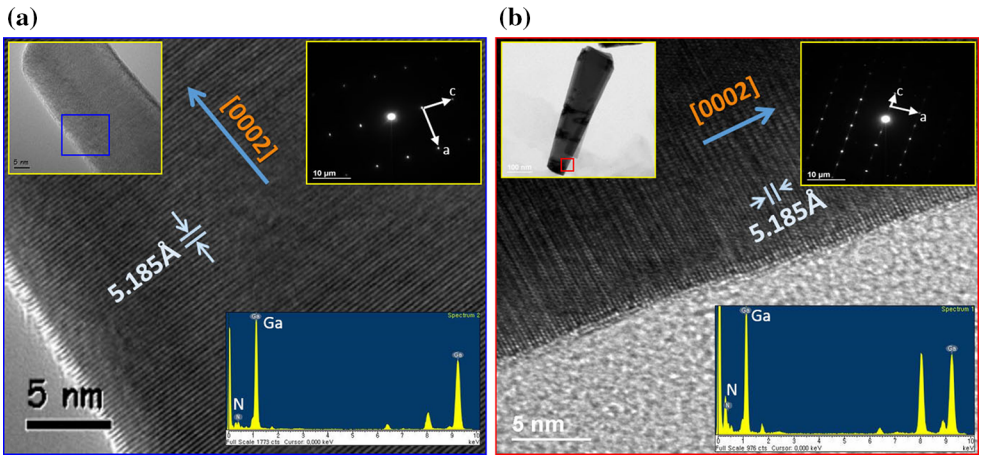

Fig. 2 X-ray diffraction patterns of the GaN nanorods grown on sapphire substrates with orientations **a** *c*-plane, **b** *a*-plane, **c** *r*-plane, and **d** *m*-plane showing growth along the different orientations. *c*- and *a*-plane sapphire shows growth along [0001] direction, *r*-plane along (110) and (103), and *m*-plane shows growth along (103)

Fig. 3 Transmission electron microscopy images of **a** *c*-plane sapphire-grown GaN nanorod and **b** *m*-plane-grown GaN nanorod. The SAD patterns in the insets confirm that the rod is single-crystalline wurtzite-structured GaN. The presence of Ga and N is evident from the EDX images in the inset

smaller diffusion barriers along the *c*-axis, than the *m*-axis. And a high Ga/N flux ratio ensures an increased Ga coverage of the surface during growth, which eventually reduces the surface anisotropy by decreasing the diffusion barrier anisotropy. Therefore, the [0001] GaN growth is favored, whereas the other orientation is suppressed on *a*-plane sapphire substrate in HVPE growth. The same is confirmed from the XRD pattern showing peaks (002) and (004) dominantly in Fig. 2b. Since the rods grown in this condition are very dense, the XRD patterns did not exhibit the peak originating from sapphire substrate.

While using *r*-plane sapphire, during the shorter nitridation of less than 1 h, the oxygen atoms are substituted for nitrogen atoms. Thereby, initially a AlN-rich interfacial zone with a thickness of two monolayers could be formed [14]. This can reduce the mismatch between the *a*-plane GaN epilayer and the *r*-plane sapphire substrates due to the misfit dislocations. Similar to the case of Nitridation in *c*-

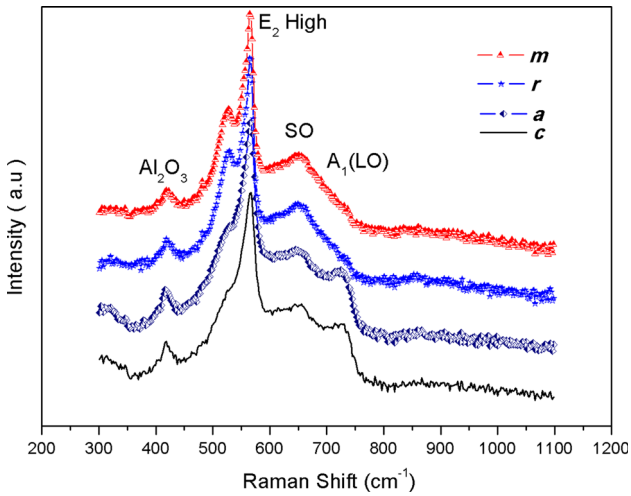

Fig. 4 Raman spectra of the semipolar and non-polar GaN nanorods (The legends *m*, *r*, *a*, and *c* represent the Al_2O_3 planes on which GaN nanorods were grown). A1 Transverse optical mode appears dominant in *m*-plane and *r*-plane, whereas A1 Longitudinal Optical mode is dominant in *c*- and *a*-plane sapphire-grown GaN

plane sapphire, here also, a parasitic semipolar (103) nanocrystals are formed, which is really a side effect [15, 16]. The epitaxial relationship is given as $[1\bar{1}20]_{n-GaN} \| [1\bar{1}02]_{Sap}$ and $[1\bar{1}00]GaN \| [1\bar{1}20]_{Sap}$. Moreover, there is larger mismatch between d-spacings of *m*-plane of GaN and *a*-plane sapphire. Because of these reasons, the growth of both orientations *a*-GaN (110) and semipolar orientation (103) occurs as shown in the SEM image, schematic, and XRD pattern in Fig. 2c.

In *m*-plane sapphire, the single semipolar $[11\bar{2}]$ GaN phase nucleates on $[10\bar{1}0]$ *m*-sapphire substrate. But in HVPE growth, it does not favor the additional growth along [0002] GaN which is found to appear in MOCVD growth. The XRD patterns in Fig. 2d show only (103) peaks, and no other additional (002) peaks. Its epitaxial relationship could be well predicted from the XRD result also. It ascertains that GaN occurs only in single orientation with a tilt angle. The tilt angle as reported by many other groups is 58.9° [17, 18]. The knowledge of the sap-

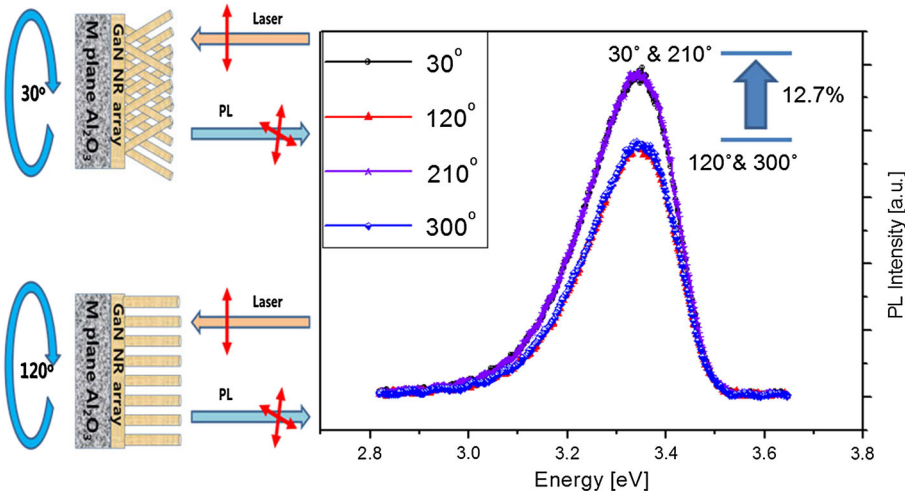

Fig. 5 Photoluminescence spectra of [11–22] inclined intertwined GaN nanorods on *m*-plane sapphire. The *left-hand side* shows the schematic variation in the incidence area, when the specimen is rotated through 0̊ to 360° in steps of 90°. The spectra show an increase in intensity of 12.7 % along 30° and 210° with that of the rest

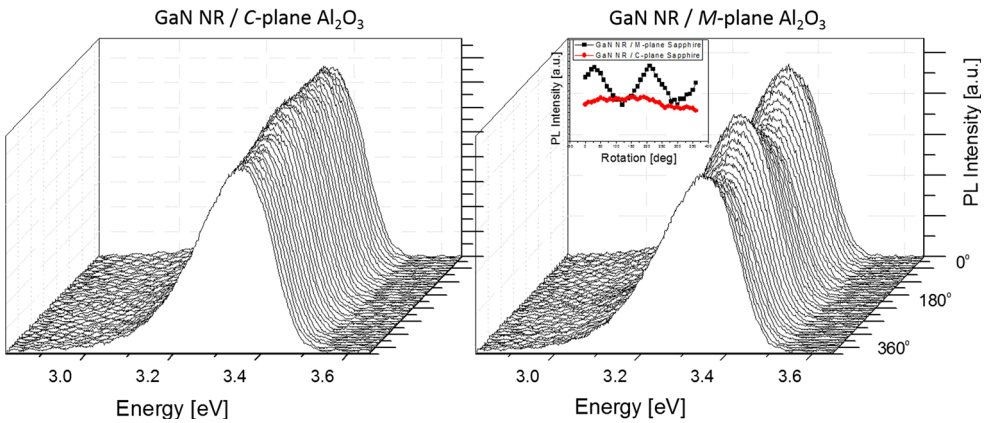

Fig. 6 Photoluminescence spectra of GaN nanorods on *c*-plane and *m*-plane GaN nanorods (measured by rotating the specimen from 0° to 360° with a step of 90°) show variations in the intensity. The inset deliberately shows the intensity variation only in the latter case, whereas *c*-plane GaN has almost the same intensity in all angles

phire crystal structures enables us a better understanding of the nucleation in this orientation. Sapphire crystallizes in a rhombohedral lattice composed of aluminum cations (Al^{3+}) and oxygen anions (O^{2-}). The positions of the anions simplify the structure to a hexagonal close-packed-like structure. The Al^{3+} cations form a two-dimensional simple square lattice on the surface, whereas the anions (O^{2-}) form zigzag rows along [0001] orientation of sapphire [19]. During Nitridation, in *m*-plane sapphire, N^{3-} is alternating along the $[0001]_{sapphire}$ direction. Therefore, only N^{3-} is only present in the regions in the place of Al^{3+}. This alternate arrangement favors only Ga^{3+} formation between two N^{3-} ions. The same arrangement continues along the Al^{3+} ion lattice on the sapphire surface. The positions of missing Al^{3+} planes along $[10\bar{1}\bar{2}]$ sapphire plane, Ga^{3+} will match sites at the interface. Therefore, the possibility of twinning orientations is prevented. The epitaxial relationship is given as $[11\bar{2}2]_{GaN} \| [10\bar{1}0]_{sapphire}$. Here, the GaN NRs are self-aligned and exhibit a inclined intertwined structure. This characteristics is applicable in polarizers and preferable in optoelectronic applications.

But, in all the above cases, GaN NRs obtained in either vertical or inclined alignment have *c*-axis as their principal axis. It is examined and verified by TEM analysis as shown in Fig. 3. The High-Resolution TEM image shows the uniform stacking of lattice along [0002] orientation having a spacing of 5.185 Å. Selected area electron diffraction pattern shown in the inset ascertains its single crystalline nature. Its composition was verified by energy dispersive X-ray analysis (EDX) which is shown in the inset as well.

Optical properties

Raman spectroscopy is an extremely active and exciting field for the benefit of science and technology. In the case of nanostructures, an increase in scattered intensity than the bulk is found in the literature which is known as Raman Antenna effect [20, 21]. Angular dependencies of the phonon modes would be possible in highly anisotropic shape of the nanowires, which are not expected from selection rules [22, 23]. Raman shifts of all the four specimens are as recorded in Fig. 4. Sharp E_2 high modes in all of the NRs confirm the high crystalline quality of the NRs grown by HVPE [24, 25].

The Raman mode, A_1 (LO) mode is symmetry-forbidden in *x* (*z*-)-*x* geometry. When the incident laser beam is not strictly perpendicular to the *c*-axis, it may allow the observation of the forbidden mode [26]. For wurtzite crystals, mixed transverse and longitudinal phonon modes appear when the propagation directions are not exactly along the principal axes [27].

The origination of peak A_1 (TO) corresponds to the ordinary excitation arising due to the arbitrary incidence angle of the exciting light. A_1 (TO) be the starting of A_1 symmetry phonon modes and this frequency corresponds to the quasi-confined modes in isolated nanowire model which are the continuation of SO modes for frequencies below A_1 (TO). TO modes will appear when the orientations have different crystalline planes [28]. TO vibration modes are exhibited when the *q* vector (propagation direction) travels in between the *c*- and *a*-planes. Therefore, A_1 (TO) modes are viable in the case of inclined NRs [29]. These modes also appear in inclined (*r*-plane grown) and intertwined (*m*-plane grown) GaN NRs wherein the *q* vector lying in between the *c*- and *a*-planes of GaN is apparent. This is not observable in the case of vertically aligned GaN NRs (both *c*-plane-grown and *a*-plane-grown cases).

Highly anisotropic shape of the NRs/nanowires can lead to angular dependencies of the phonon modes. Normally, SO modes are observed when the translational symmetry of the SO potential is broken. This breakdown of symmetry can activate a larger wave vector SO mode whose frequency is sufficiently separated from the other Raman-active optical phonons. The SO mode is associated with the surface modulation in GaN. In this case, the non-polar and semipolar growths which are different from the *c*- and *a*-axis growths cause the surface modulation which may give rise to SO modes [30].

The PL spectrum of $[11\bar{2}2]$ GaN NRs with an angular rotation of the sample, from 0° to 360° in steps of 10°, was measured in order to study its polarizing property. Figure 5 shows the variation in intensity at different angles. It shows an increase in intensity up to 12.7 % along the angles 30° and 210°. In the PL analysis, the polarized He–Cd laser beam is likely to be incident on the inclined intertwined GaN NRs, and the area of excitation varies depending upon the axial and radial surfaces of the NRs. In the case of axial incidence and excitation, the area excited is more at certain angles (30° and 210°) and lesser at certain other angles (120° and 300°). The intensity variation is attributed to this variation in area of excitation which is shown in Fig. 6 [31]. The *c*-plane sapphire shows a same intensity irrespective of the angle of rotation. Therefore, the maxima and minima in the intensity are due to the larger and smaller exposed areas of the NRs.

Conclusions

GaN NRs are grown on different orientations of sapphire like [0001] *c*-plane, $[11\bar{2}0]$*a*-plane, $[1\bar{1}02]$ *r*-plane, and $1\bar{1}00$ *m*-plane substrates by hydride vapor phase epitaxy. The obtained NRs by XRD analysis and electron microscopy analysis are found to be vertically aligned in the *c*-plane and *a*-plane sapphire with [0001] GaN. But in *r*-plane and *m*-plane sapphire, the orientations are found to be tilted

skew [(110) and semipolar orientation (103)] and inclined intertwined $[11\bar{2}2]$ GaN NRs, respectively. The growth conditions and the epitaxial relationships were discussed in detail. A detailed TEM analysis confirms that all the NRs when separated from the substrate have the characteristic *c*-axis orientation in all the cases. Raman spectroscopy exhibits A_1 (LO) modes in vertically aligned GaN NRs, and A_1 (TO) modes in inclined GaN NRs. SO of Raman shift was observed in all the cases. The difference in the optical behaviors has been reasoned out with suitable evidences. The azimuth-dependent PL spectra show increased intensity along 30° and 210° than that along other angles which is attributed to the change in the incident excited area by the polarized laser beam along the axial and radial surfaces of the inclined NRs, but does not vary in the case of vertically aligned ones. The prepared non-polar GaN NRs are suitable for applications in polarizers. A detailed study of growth of GaN NRs HVPE on different orientations of sapphire substrates was carried out. The epitaxial relationship of the formed GaN NRs is investigated and reasons are explained.

Acknowledgements This research was supported by Leading foreign Research institute recruitment Program through the National foundation of Korea (NRF) funded by the ministry of education, Science and Technology (MEST) (No. 2014-039452) and by the International Research & Development Program of the National Research Foundation of Korea (NRF) funded by the Ministry of Education, Science and technology (MEST) of Korea (No. 2014-073957).

References

1. Kim H-M, Lee H, Kim SI, Ryu SR, Kang TW, Kim DY, Kwan SC, Jin PH, Woo YD (2004) Field emission properties of needle shaped gan nanorod arrays. J Korean Phys Soc 45:S701–S703
2. Kim HM, Cho YH, Lee HS, Kim SI, Ryu SR, Kim DY, Kang TW, Chung KS (2004) High-brightness light emitting diodes using dislocation-free indium gallium nitride/gallium nitride multi quantum-well nanorod arrays. Nano Lett 4:1059–1062
3. Zhang XM, Lu MY, Zhang Y, Chen LJ, Wang ZL (2009) Fabrication of a high-brightness blue-light-emitting diode using a zno-nanowire array grown on p-gan thin film. Adv Mater 21:2767–2770
4. Chierchia R, Boettcher T, Heinke H, Einfeldt S, Figge S, Hommel D (2003) Microstructure of hetero epitaxial GaN revealed by X-ray diffraction. J Appl Phys 93:8918–8925
5. Grahn HT (2007) Optical polarization anisotropies in GaN films for different nonpolar orientations. Phys Status Solidi B 244:1839–1847
6. Armitage R, Hirayama H (2008) M-plane GaN grown on m-sapphire by metalorganic vapor phase epitaxy. Appl Phys Lett 92:092121–092123
7. Kelzenberg MD, Boettcher SW, Petykiewicz JA, Turner-Evans DB, Putnam MC, Warren EL, Spurgeon JM, Briggs RM, Lewis NS, Atwater AH (2010) Enhanced absorption and carrier collection in Si wire arrays for photovoltaic applications. Nat Mater 9:239–244
8. Tessarek C, Figge S, Gust A, Heilmann M, Dieker C, Spiecker E, Christiansen S (2014) Optical properties of vertical, tilted and in-plane GaN nanowires on different crystallographic orientations of sapphire. J Phys D 47:394008–394017
9. Zhu T, Martin D, Grandjean N (2009) M-Plane GaN Grown on m-Plane Sapphire by Hydride Vapor Phase Epitaxy. Jpn J Appl Phys 48:020226–020228
10. Chae SR, Lee KS, Jang JJ, Min DH, Kim JH, Nam OH (2105) Self-assembled growth of inclined GaN nanorods on (10–10) m-plane sapphire using metal–organic chemical vapor deposition. J Cryst Growth 409:65–70
11. Kim HM, Lee HS, Kim SI, Ryu SR, Kang TW, Chung KS (2004) Formation of InGaN nanorods with indium mole fractions by hydride vapor phase epitaxy. Phys Status Solidi B 241:2802–2805
12. Basha SM, Ryu SR, Kang TW, Srivastava ON, Ramakrishnan V, Kumar J (2012) Effect of growth temperature on gallium nitride nanostructures using HVPE technique. Phys E 44:1885–1888
13. Konenkova EV, Zhilyaev YV, Fedirko VA, Zahn DRT (2003) Raman spectroscopy of GaN nucleation and free-standing layers grown by hydride vapor phase epitaxy on oxidized silicon. Appl Phys Lett 83:629–631
14. Felice R, Northrup JE (1998) Energetics of AlN thin films on the Al2O3 (0001) surface. Appl Phys Lett 73:936–938
15. Koziorowska JS, Komninou P, Sahonta SL, Kioseoglou J, Tsiakatouras G, Georgakilas A (2008) Electron microscopy investigation of extended defects in a-plane gallium nitride layers grown on r-plane sapphire by molecular beam epitaxy. Phys Status Solidi C 5:3748–3751
16. Koziorowska JS, Tsiakatouras G, Lotsari A, Gergakilas A, Dimitrakopulos GP (2010) The defect character of GaN growth on r-plane sapphire. J Appl Phys 107:073525–073534
17. Kappers MJ, Hollander JL, Aleese CM, Johnson CF, Broom RF, Barnard JS, Vickers ME, Humphreys CJ (2007) Growth and characterisation of semi-polar (11–22) InGaN/GaN MQW structures. J Cryst Growth 300:155–159
18. Vennegues P, Bougrioua Z, Guehne T (2007) Microstructural characterization of semipolar GaN templates and epitaxial-lateral-overgrown films deposited on m-plane sapphire by metalorganic vapor phase epitaxy. Jpn J Appl Phys 46:4089–4095
19. Frentrup M, Ploch S, Pristovsek M, Kneissl M (2011) Crystal orientation of GaN layers on (10–10) m-plane sapphire. Phys Status Solidi B 248:583–587
20. Xiong Q, Chen G, Gutierrex HR, Eklund PC (2006) Raman scattering as a probe of phonon confinement and surface optical modes in semiconducting nanowires. Appl Phys A 85:299–305
21. Cao LY, Laim L, Valenzuela PD, Nabet B, Spanier JE (2007) On the Raman scattering from semiconducting nanowires. J Raman Spectrosc 38:697–703
22. Pauzauskie PJ, Talaga D, Seo K, Yang PD, Lagugne-Labarthet F (2005) Polarized Raman confocal microscopy of single gallium nitride nanowires. J Am Chem Soc 127:17146–17147
23. Nobile C, Fonoberov VA, Kudera S, Torre AD, Ruffino A, Chilla G, Kipp T, Heitmann D, Manna L, Cingolani R, Balandin AA, Krahne R (2007) Confined optical phonon modes in aligned nanorod arrays detected by resonant inelastic light scattering. Nano Lett 7:476–479
24. Tu LW, Hsiao CL, Chi TW, Lo I, Hsieh KY (2003) Self-assembled vertical GaN nanorods grown by molecular-beam epitaxy. Appl Phys Lett 82:1601–1603
25. Hsiao CL, Tu LW, Chi TW, Chen M, Young YF, Chia CT, Chang YM (2007) Micro-Raman spectroscopy of a single freestanding GaN nanorod grown by molecular beam epitaxy. Appl Phys Lett 90:043102
26. Koh EK, Park IW, Choi H, Yoon M, Choh SH, Kim HS, Cho YM, Kim S, Park SS (2005) Depth-dependent optical properties

of a HVPE-grown freestanding Si-doped GaN single crystal. J Cryst Growth 276:37–42
27. Zhang JM, Ruf T, Cardona M, Ambacher O, Stutzmann M, Wagner JM, Bechstedt F (1997) Raman spectra of isotopic GaN. Phys Rev B 56:14399–14406
28. Dhara S, Das CR, Hsu HC, Raj B, Bhaduri AK, Chen LC, Chen KH, Albert SK, Ray A (2008) Recrystallization of epitaxial GaN under indentation. Appl Phys Lett 92:143114–143116
29. Bergman L, Dutta M, Balkas C, Davis RF, Christman AJ, Alexson D, Memanich RJ (1999) Raman analysis of the E1 and A1 quasi-longitudinal optical and quasi-transverse optical modes in wurtzite AlN. J Appl Phys 85:3535–3539
30. Sahoo S, Dhara S, Dash S, Tyagi AK, Raj B, Das CR, Chandramohan P, Srinivasan MP (2010) Surface optical modes in GaN nanowires. Int J Nanotechnol 7:823–832
31. Chen HY, Yang YC, Lin HW, Chang SC, Gwo S (2008) Polarized photoluminescence from single GaN nanorods: effects of optical confinement. Opt Express 16:13465–13475